RSC Advances

PAPER

View Article Online
View Journal | View Issue

Open Access Article. Published on 20 February 2017. Downloaded on 12/10/2025 8:27:51 AM.
This article is licensed under a Creative Commons Attribution-NonCommercial 3.0 Unported Licence.

Cite this: *RSC Adv.*, 2017, **7**, 12027

A simple route to prepare a Cu_2O–CuO–GN nanohybrid for high-performance electrode materials†

Yanyun Liu,*[a] Ling Ma,[a] Dong Zhang,[b] Gaoyi Han[cd] and Yunzhen Chang[cd]

Received 9th November 2016
Accepted 9th February 2017

DOI: 10.1039/c6ra26535a

rsc.li/rsc-advances

Cu_2O–CuO–GN nanohybrid is prepared by a simple electrochemical method by applying a positive and negative pulse electric signal on a dispersion of a mixture of GO and $Cu(NO_3)_2$. During the process, reduction of graphene oxide and deposition of Cu_2O–CuO on GN occur simultaneously. The nanohybrid is systematically characterized by X-ray diffraction (XRD), X-ray photoelectron spectroscopy (XPS), scanning electron microscopy (SEM) and transmission electron microscopy (TEM). Cu_2O–CuO nanoparticles with diameters around 100 nm are uniformly distributed on the GN. In addition, the electrochemical properties of the Cu_2O–CuO–GN nanohybrid are investigated by cyclic voltammetry (CV), galvanostatic charge/discharge (DC) and electrochemical impedance spectrometry measurements (EIS). The Cu_2O–CuO–GN nanohybrid shows a higher specific capacitance (222 F g^{-1} at 1 A g^{-1}) than that of pure GN (143 F g^{-1} at 1 A g^{-1}) prepared under the same conditions. This approach opens up the possibility for fabrication of high-performance GN-based electrode materials.

1. Introduction

Graphene (GN), a two-dimensional one-atom thick carbon, has attracted increasing attention in the past several years, mainly due to its outstanding electronic, thermal, and mechanical properties.[1–4] Such superior performances endow it with exceptional application potential in many fields including catalysis,[5] sensors,[6,7] adsorption,[8] energy storage,[9,10] and so on. However, the exceptional inherent properties of GN are often reduced by GN aggregation and stacking, which is driven by the strong π–π interactions between individual GN sheets.[11] In addition, the quality of GN is hardly controllable due to abundant chemical defects formed in the synthetic process. Therefore, the prevention of restacking and the reduction of chemical defects from GN has been a significant issue in developing GN-based electrochemical materials.

The addition of extra additives during the GN preparation process has been reported, and is demonstrated to overcome the above mentioned issues. Thus, various GN based composites have been widely reported in the electrochemical application, such as transition metal oxide nanoparticles/GN,[12] carbon nanomaterials/GN,[13–15] conducting polymer/GN,[16] *etc.* Actually, the extra additive deposited on the surface of GN as a nanospacer can restrain the restacking of GN during the reduction of graphene oxide (GO). Moreover, GN not only offers a 2D conductive backbone for the rapid electron transport, but also allows the decoration by uniform additives to facilitate the utilization of electrode materials.

Among the transition metal oxides, Cu_2O, CuO have the unique optical and good electrochemical properties,[17–22] which makes it a promising candidate in many applications, such as supercapacitors,[23] solar-energy conversion devices,[24] and lithium-ion batteries,[25] *etc.* Up to now, Cu_2O/GN and CuO/GN nanohybrid have been synthesized by various methods. For example, Wang *et al.* synthesized Cu_2O/CuO/GN nanohybrid through a hydrothermal-assisted reaction.[26] Zhu *et al.* synthesized CuO/GN composite through *in situ* chemical synthesis approach.[27] However, these mentioned methods still have the unsolved problems for regarding Cu_2O/CuO decoration of GN: (1) the adopted chemical ways are usually complicated using numerous reducing, precipitating, and stabilizing agents.[28–30] (2) It is still a challenge to achieve the convenient production of Cu_2O/GN and CuO/GN composites. To overcome these shortcomings, we used a one-pot electrochemical method to prepare Cu_2O–CuO–GN nanohybrid. The electrochemical method is a well developed and economical method that has been successfully applied for the deposition of carbon nanotubes and GO particles.[31,32]

In this paper, Cu_2O–CuO–GN nanohybrid is prepared by applying positive and negative pulse electric signal on GO and

[a]College of Chemistry and Chemical Engineering, Jinzhong University, Jinzhong 030619, PR China. E-mail: 312217642@qq.com
[b]School of Material Science and Engineering, Tongji University, Shanghai 200092, PR China
[c]Institute of Molecular Science, Innovation Center of Chemistry and Molecular Science, Shanxi University, Taiyuan 030006, PR China
[d]Key Laboratory of Materials for Energy Conversion and Storage of Shanxi Province, Taiyuan 030006, PR China

† Electronic supplementary information (ESI) available. See DOI: 10.1039/c6ra26535a

Open Access Article. Published on 20 February 2017. Downloaded on 12/10/2025 8:27:51 AM.
This article is licensed under a Creative Commons Attribution-NonCommercial 3.0 Unported Licence.

$Cu(NO_3)_2$ mixture dispersion. During the process, reduction of graphene oxide and deposition of nano-Cu_2O/nano-CuO on GN occur simultaneously. Our green synthesis approach avoids using harsh, toxic and explosive chemicals such as hydrazine hydrate and sodium borohydride for reducing GO. The electrochemical behavior of as-prepared Cu_2O–CuO–GN nanohybrid is examined by cyclic voltammetry (CV) and galvanostatic charge/discharge (DC) and electrochemical impedance spectrometry measurements (EIS). The results show that this method is simple to provide Cu_2O–CuO–GN nanohybrid for high-performance electrode materials.

2. Experimental

2.1 Materials and instrument

The graphite oxide was prepared according to the method developed by Hummers' and Offemann,[33] and all other chemicals used in this study were of analytical grade. Signal generator (DG1022) and Oscilloscope (DS1052E) were purchased from Beijing Puyuan Technologies Co., Power amplifier (HVP-300A) was bought from Nanjing FonanCo.

2.2 Preparation of GN and Cu_2O–CuO–GN

The suspension of graphene oxide (GO, 1 mg mL^{-1}) was prepared by dispersing the graphite oxide powder into water with the help of ultrasonication for 2 h. A 1 mL $Cu(NO_3)_2$ solution with a concentration of 0.1 mol L^{-1} was introduced into the as-prepared GO suspension under ultrasonication. Then the mixture suspension was loaded in a glass container. Copper electrodes were used in the experiment. The electrode separation was 10 millimeters. Positive and negative pulse signal whose frequency and peak-to-peak voltage (V_{pp}) were 5 Hz and 20 V respectively were applied on the electrodes in the mixture dispersion. This signal was produced by the signal generator and amplified by the power amplifier. Electrode which adsorbed thick film was taken out after 2 h and dried in the air. Then flexible Cu_2O–CuO–GN thin film was obtained by peeling off from the electrodes and cut by a razor blade into rectangular strips for testing without further modification. For comparison, GN was prepared using the same procedure without adding $Cu(NO_3)_2$ solution.

2.3 Characterization

The X-ray diffraction (XRD) patterns of samples were obtained by using a D8 Cu Kα radiation (D/max 2550VB3+/PC, Rigaku, Japan). The microstructures and morphology of samples were observed with a field emission scanning electron microscopy (SEM, Quanta 200FEG, FEI) and transmission electron microscope (TEM, JEM-2100F). X-ray photoelectron spectroscopy (XPS) analysis were performed with an ESCALAB 250Xispectrometer (Thermo Electron) using a monochromic Al Kα source at 1486.6 eV.

2.4 Electrochemical measurements

The fabrication of the supercapacitors is described as follows: two nearly identical Cu_2O–CuO–GN (GN) samples were separated by a filter paper soaked with 1.0 mol L^{-1} KCl aqueous solution. Before the electrochemical measurements, the slices of samples were also immersed in KCl aqueous solution under vacuum in order to exchange their interior water with electrolyte. Two foam nickels were used as the flexible current collectors. All the components were assembled into a sandwiched structure between the two substrates. Electrochemical performances of the supercapacitors were tested by CV, DC, EIS measurements on a CHI660E electrochemistry workstation (Chenhua, Shanghai). Potential windows for the CV measurements and DC tests ranged from −0.5 to 0.5 V. EIS tests were carried out in the frequency range of 10^5 to 0.1 Hz at the amplitude of 5 mV, referring to open circuit potential. The specific capacitance (C_{sc}) of the electrodes was calculated based on DC curves:

$$C_{sc} = 2I\Delta t/\Delta Vm$$

where I represents the constant discharge current, Δt the discharging time, m the mass of one electrode, and ΔV the voltage drop upon discharging.

3. Results and discussion

X-ray diffraction (XRD) pattern of as-synthesized Cu_2O–CuO–GN indicates the mixed phase of Cu_2O and CuO (Fig. 1). For Cu_2O–CuO, diffraction peaks centered at $2\theta = 28°$, 33°, 43° and 62° correspond to the (110), (111), (200) and (220) crystal planes of Cu_2O, respectively. Moreover, the peaks located at 37°, 43°, 51°, and 74° can be assigned to the (110), (111), (200), and (220) planes of CuO, respectively. Both of these results suggest the presence of both Cu_2O and CuO in the sample.

SEM represents the morphology of the sample surface. SEM images of GN and Cu_2O–CuO–GN nanocomposite are presented in Fig. 2(a) and (b). It is clearly seen that the as-prepared GN exhibits typical wrinkled structures which prevent the sheets from stacking into dense structure. The wrinkled structures of GN could provide suitable sites for deposition of Cu_2O–CuO. Cu_2O–CuO–GN shows the formation of flakes composed of the small nanoparticles. It is seen that Cu_2O–CuO nanoparticles are

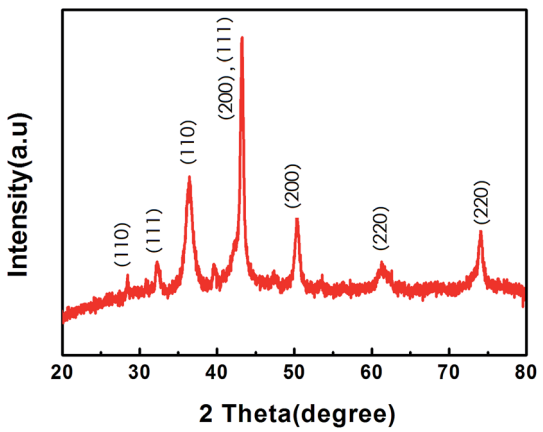

Fig. 1 XRD pattern of Cu_2O–CuO–GN nanohybrid.

This journal is © The Royal Society of Chemistry 2017

Open Access Article. Published on 20 February 2017. Downloaded on 12/10/2025 8:27:51 AM.
This article is licensed under a Creative Commons Attribution-NonCommercial 3.0 Unported Licence.

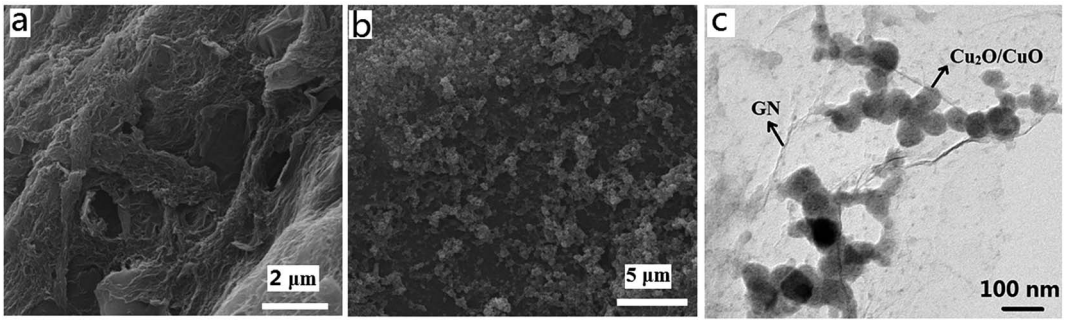

Fig. 2 SEM images of GN (a) and Cu_2O–CuO–GN (b), TEM image of Cu_2O–CuO–GN (c).

uniformly dispersed on the surface of GN. Fig. 2c shows TEM image of Cu_2O–CuO–GN nanocomposite. The image indicates that the diameters of nanoparticles are around 100 nm.

The XPS is one of best methods to investigate the chemical composition and electronic structure of the Cu_2O–CuO–GN. Fig. 3 shows the wide scan and deconvoluted XPS spectra of Cu_2O–CuO–GN and GO (a–d). The elements of Cu, C, and O were clearly observed in Fig. 3(a). Fig. 3(b) and (c) show both the C 1s XPS spectra of GO and Cu_2O–CuO–GN. Four different peaks centered at 284.0 eV (C=C), 284.5 eV (C–C), 286.3 eV (C–O) and 288.1 eV (O=C) were detected in GO sample (Fig. 2b). After reaction, the intensities of all C 1s peaks of the carbons binding to oxygen decreased dramatically, revealing that the deoxygenation process accompanied the reduction of GO in the

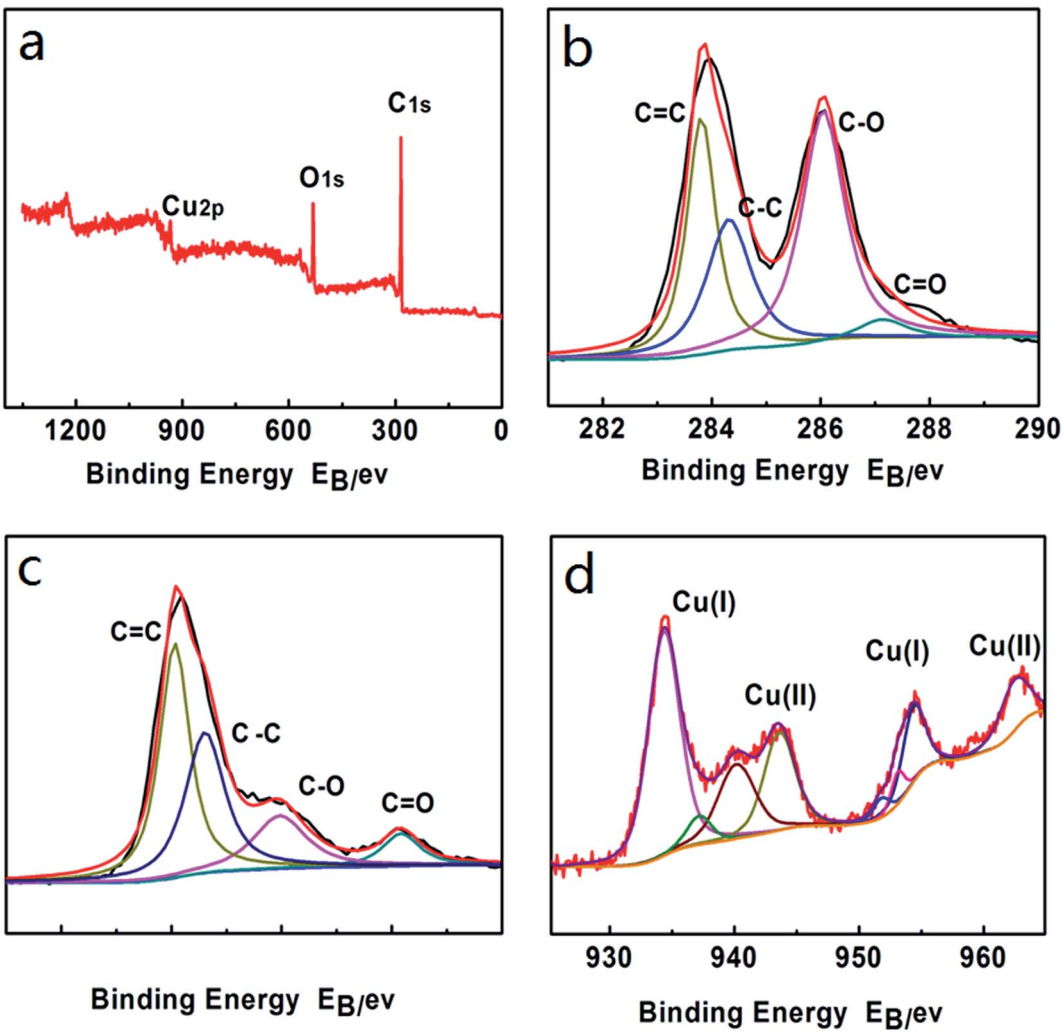

Fig. 3 Wide scan XPS spectra of Cu_2O–CuO–GN (a), deconvoluted XPS spectra of GO (b) and Cu_2O–CuO–GN (c and d).

Open Access Article. Published on 20 February 2017. Downloaded on 12/10/2025 8:27:51 AM.
This article is licensed under a Creative Commons Attribution-NonCommercial 3.0 Unported Licence.

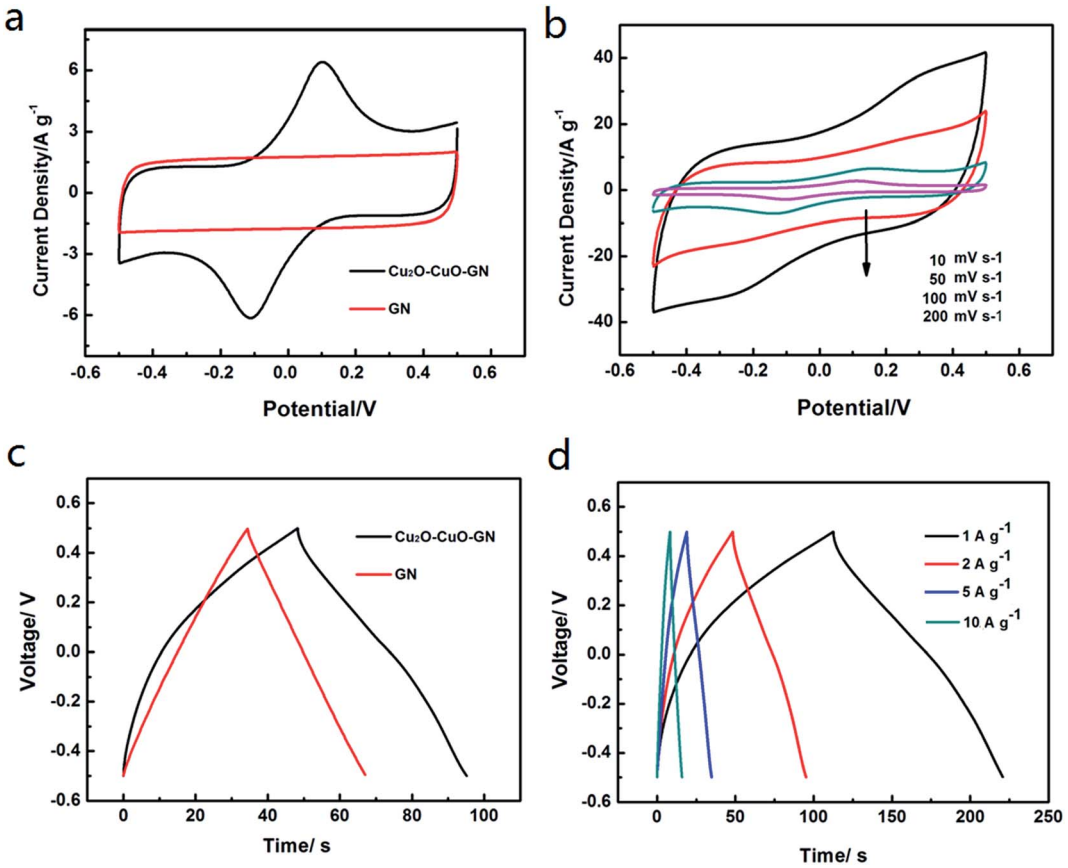

Fig. 4 (a) CV curves of GN and Cu_2O–CuO–GN at scan rate of 10 mV s^{-1}. (b) CV curves of Cu_2O–CuO–GN at different scan rates. (c) DC curves of GN and Cu_2O–CuO–GN at current density of 2.0 A g^{-1}. (d) DC curves of Cu_2O–CuO–GN at various current densities.

electrochemical reaction. The oxidation state of Cu has also been investigated using XPS (Fig. 3d) and shows the presence of a mixture of oxidation states such as Cu(I) and Cu(II). The result suggests the presence of both Cu_2O and CuO in the sample. In this experiment, GO platelets migrated toward the working electrode as soon as a positive pulse was applied. Then these deposited platelets were reduced, meanwhile, Cu_2O–CuO nanoparticles deposited on the surface of GN when a negative pulse was applied. The possible reactions are as follow:

$$\text{Positive pulse: } 4H^+ + 2GO + 4e^- = 2GN + 2H_2O$$

$$\text{Negative pulse: } 2Cu^{2+} + 2e^- + 2OH^- = Cu_2O + H_2O$$

$$Cu^{2+} + 2OH^- = CuO + H_2O$$

Fig. 4a shows CV curves of Cu_2O–CuO–GN and GN at a scan rate of 10 mV s^{-1}. It can be seen that the curve of Cu_2O–CuO–GN electrode has a rectangular-like shape with a broad redox peaks, indicating the contribution of both EDLC behavior and pseudocapacitive characteristics. The curve of Cu_2O–CuO–GN displays a pair of redox peaks which can be attributed to reversible Cu(I)/Cu(II) redox reactions involving one electron transfer process. The mechanism of redox reactions occurring at the Cu_2O–CuO–GN electrode can be proposed as:[34]

$$Cu^{2+} + e^- \rightarrow Cu^+$$

The CV of GN exhibits a symmetric rectangular shape, indicating an ideal electric double layer capacitive behavior. Also, the current density of Cu_2O–CuO–GN nanohybrid is higher than that of GN due to the positive effect of Cu_2O–CuO on energy storage capability.

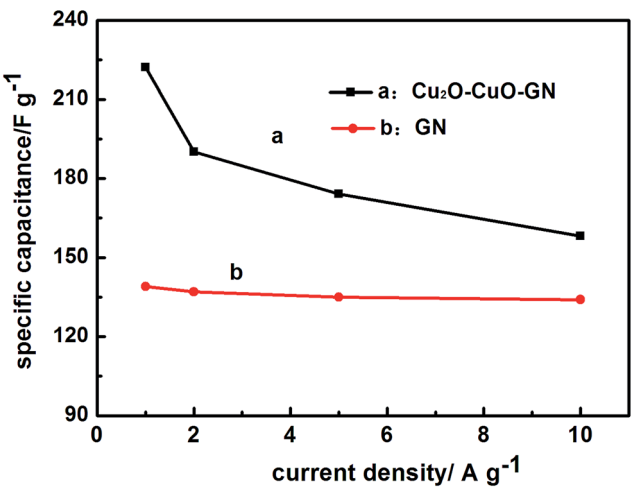

Fig. 5 The relationships between C_s and current densities.

This journal is © The Royal Society of Chemistry 2017

Open Access Article. Published on 20 February 2017. Downloaded on 12/10/2025 8:27:51 AM.
This article is licensed under a Creative Commons Attribution-NonCommercial 3.0 Unported Licence.

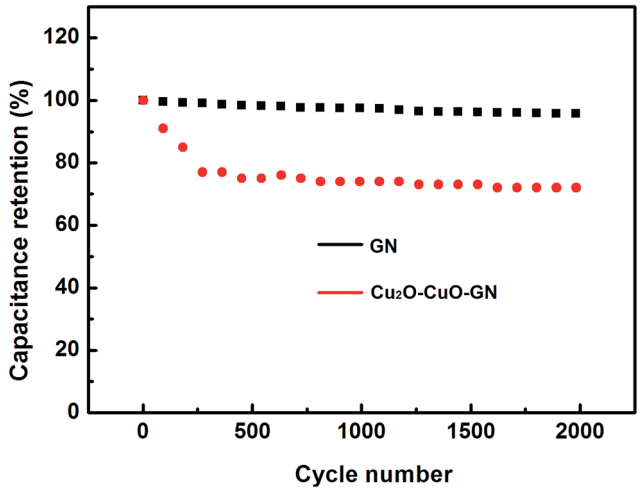

Fig. 6 Comparison of cycle performance of GN and Cu_2O–CuO–GN.

Fig. 4b displays the CV curves of the Cu_2O–CuO–GN electrode at different scan rates. The prominent increase of the current is observed by increasing scan rate which indicates the capacitive behavior of Cu_2O–CuO–GN electrode. During the increasing scan rates, inner active sites cannot completely contribute in the redox transitions and the capacitance of the electrode decreases. Also, the redox peaks tend to disappear with increasing scan rate, suggesting a kinetic limitation for the reaction between the redox sites at scan rate beyond 200 mV s^{-1}. Moreover, anodic and cathodic peaks shift towards the positive and negative potentials, respectively, which is due to the resistance of the electrode. Fig. 4c shows the DC curves of Cu_2O–CuO–GN and GN electrodes at a current density of 2 A g^{-1}. The curve of GN electrode shows a typical triangular symmetrical distribution, indicating that GN has good electro-chemical double-layer capacitive behavior, which is in agreement with the results obtained from the CV curve. The Cu_2O–CuO–GN electrode exhibits a nonlinear discharge–charge curve, the typical behaviors of the combination of EDLC of GN and pseudocapacitance from the redox reaction of Cu_2O–CuO. On the basis of the DC curves, it can be concluded that covering the Cu_2O–CuO nanoparticles on the GN network can introduce new paths for electron transfer and therefore improve the conductivity and capacitance behavior of the electrodes. Providing intact contact between the thin GN sheets and the Cu_2O–CuO nanoparticles in a molecular scale, the composite material Cu_2O–CuO–GN showed higher capacitance than those of pure GN. In addition, the electrochemical behaviors of GN and Cu_2O–CuO–GN were also analyzed by using a three-electrode system, in which a platinum disk was used as the counter electrode and a saturated calomel electrode was used as the reference electrode (see ESI†).

To further examination the rate capability of the Cu_2O–CuO–GN nanohybrid, DC experiments were performed at different current densities, as shown in Fig. 4d. At high current densities, inner active sites cannot contribute in the redox transitions due to the diffusion effect of ions within the electrode. The variations of C_s at different current densities were shown in Fig. 5. When the current densities were increased up to 10 A g^{-1}, the Cu_2O–CuO–GN and GN electrodes maintained nearly 72% and 96% of their initial C_s values, respectively. At a given current density, *e.g.*, 1 A g^{-1}, the C_s of electrode was 222 F g^{-1} for Cu_2O–CuO–GN, larger than 143 F g^{-1} for GN. Cycle ability is another important criterion to evaluate the compatibility during prolonged cycling. In this regard, GN and Cu_2O–CuO–GN were cycled at current density of 2 A g^{-1} and the cycling profiles are given in Fig. 6. The capacitances of the Cu_2O–CuO–GN supercapacitor show a decrease during the first 200 cycles and then keep stable. The capacitance remains about 72% of its initial values after 2000 cycles, indicating that Cu_2O–CuO–GN is a suitable nanohybrid in practical energy storage systems.

The electrochemical performance of the Cu_2O–CuO–GN and GN were further explored by EIS measurements, the results were shown in Fig. 7A along with an equivalent circuit model (Fig. 7B). Here, R_s is the total resistance of electrolyte, electrode, current collector and separator. C and R_{ct} are the capacitance and charge transfer resistance. W is the Warburg impedance related to the diffusion/transport of ions in the electrolyte to the surface of the electrode. The impedance spectrum is characterized by a well-defined semicircle at high and intermediate frequencies and a straight line inclined at a constant angle

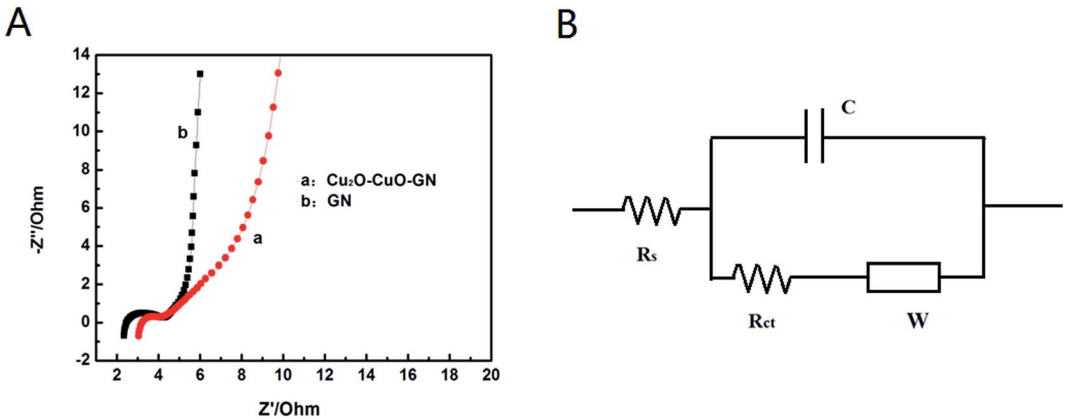

Fig. 7 (A) Nyquist plot of GN and Cu_2O–CuO–GN (B) corresponding equivalent circuit used for Nyquist plot simulation.

Open Access Article. Published on 20 February 2017. Downloaded on 12/10/2025 8:27:51 AM. This article is licensed under a Creative Commons Attribution-NonCommercial 3.0 Unported Licence.

relative to the real axis at low frequencies. The high-frequency semicircle corresponds to the equivalent series internal resistance, while the semicircle in the medium-frequency region represents the charge-transfer resistance at the electrode/electrolyte interface. The inclined line is associated with ions diffusion within the electrode materials. After fitting the impedance spectrum, the internal resistance value of Cu_2O–CuO–GN electrode was found to be 2.8 Ω. This value was very close to the GN electrode (2.3 Ω). All of those illustrated that the material of Cu_2O–CuO–GN may be developed as a suitable material for electrochemical capacitors applications.

4. Conclusions

In summary, we have demonstrated a simple and efficient electrochemical method for preparing Cu_2O–CuO–GN nanohybrid by applying positive and negative pulse electric signal on GO and $Cu(NO_3)_2$ mixture dispersion. XRD pattern of nanohybrid confirms the formation of Cu_2O–CuO loaded on the ERGO. TEM and SEM image analysis reveals the successful decoration of GN with Cu_2O–CuO. In addition, the Cu_2O–CuO–GN nanohybrid shows a higher specific capacitance (222 F g^{-1} at 1 A g^{-1}) than that of pure GN (143 F g^{-1} at 1 A g^{-1}) prepared under the same conditions. Therefore, this method is a promising candidate to provide Cu_2O–CuO–GN nanohybrid for high-performance GN-based electrode materials.

Acknowledgements

Financial support was provided by the Doctoral Startup and Research Fund (BSJJ2015212) of Jinzhong University, the Foundation of Key Laboratory of Materials for Energy Conversion and Storage of Shanxi Province (MECS2016001).

References

1 K. S. Novoselov, A. K. Geim, S. V. Morozov, D. Jiang, Y. Zhang, S. V. Dubonos, *et al.*, *Science*, 2004, **306**, 666.
2 A. K. Geim, *Science*, 2009, **324**, 1530.
3 C. Lee, X. Wei, J. W. Kysar and J. Hone, *Science*, 2008, **321**, 385.
4 A. A. Balandin, S. Ghosh, W. Bao, I. Calizo, D. Teweldebrhan, F. Miao, *et al.*, *Nano Lett.*, 2008, **8**, 902.
5 D. Deng, K. S. Novoselov, Q. Fu, N. Zheng, Z. Tian and X. Bao, *Nat. Nanotechnol.*, 2016, **11**, 218.
6 H. Sun, L. Wu, W. Wei and X. Qu, *Mater. Today*, 2013, **16**, 433.
7 S. S. Varghese, S. Lonkar, K. K. Singh, S. Swaminathan and A. Abdala, *Sens. Actuators, B*, 2015, **218**, 160.
8 J. Xu, L. Wang and Y. Zhu, *Langmuir*, 2012, **28**, 8418.
9 M. Pumera, *Energy Environ. Sci.*, 2011, **4**, 668.
10 D. A. C. Brownson, D. K. Kampouris and C. E. Banks, *J. Power Sources*, 2011, **196**, 4873.
11 X. Wang, G. Sun, P. Routh, D. H. Kim, W. Huang and P. Chen, *Chem. Soc. Rev.*, 2014, **43**, 7067.
12 W. Zhang, B. Quan, C. Lee, S. K. Park, X. Li, E. Choi, G. Diao and Y. Piao, *ACS Appl. Mater. Interfaces*, 2015, **7**, 2404.
13 W. Zhang, M. Chen, X. Gong and G. Diao, *Carbon*, 2013, **61**, 154.
14 B. You, L. Wang, L. Yao and J. Yang, *Chem. Commun.*, 2013, **49**, 5016.
15 C. Zhu, J. Zhai and S. Dong, *Nanoscale*, 2014, **6**, 10077.
16 N. A. Kumar and J. B. Baek, *Chem. Commun.*, 2014, **50**, 6298.
17 H. Zhang, J. Feng and M. Zhang, *Mater. Res. Bull.*, 2008, **43**, 3221.
18 K. X. Yao, X. M. Yin, T. H. Wang and H. C. Zeng, *J. Am. Chem. Soc.*, 2010, **132**, 6131.
19 Y. Li, S. Chang, X. Liu, J. Huang, J. Yin, G. Wang and D. Cao, *Electrochim. Acta*, 2012, **85**, 393.
20 G. H. Dong, Z. H. Ai and L. Z. Zhang, *Water Res.*, 2014, **66**, 22.
21 D. Y. Fu, G. Y. Han, Y. Z. Chang and J. H. Dong, *Mater. Chem. Phys.*, 2012, **132**, 673.
22 W. Lv, F. Sun, D. M. Tang, H. T. Fang, C. Liu, Q. H. Yang and H. M. Cheng, *J. Mater. Chem.*, 2011, **21**, 9014.
23 C. Dong, Y. Wang, J. Xu, G. Cheng, W. Yang, T. Kou, Z. Zhang and Y. Ding, *J. Mater. Chem. A*, 2014, **2**, 18229.
24 Y. S. Lee, D. Chua, R. E. Brandt, S. C. Siah, J. V. Li, J. P. Mailoa, S. W. Lee, R. G. Gordon and T. Buonassisi, *Adv. Mater.*, 2014, **26**, 4704.
25 D. Liu, Z. Yang, P. Wang, F. Li, D. Wang and D. He, *Nanoscale*, 2013, **5**, 1917.
26 K. Wang, X. Dong, C. Zhao, X. Qian and Y. Xu, *Electrochim. Acta*, 2015, **152**, 433.
27 J. Zhu, G. Zeng, F. Nie, X. Xu, S. Chen, Q. Han and X. Wang, *Nanoscale*, 2010, **2**, 988.
28 C. Xu, X. Wang, L. Yang and Y. Wu, *J. Solid State Chem.*, 2009, **182**, 2486.
29 Y. Yang, C. Tian, J. Wang, L. Sun, K. Shi, W. Zhou and H. Fu, *Nanoscale*, 2014, **6**, 7369.
30 H. Meng, W. Yang, K. Ding, L. Feng and Y. Guan, *J. Mater. Chem. A*, 2015, **3**, 1174.
31 S. Pei, J. Du, Y. Zeng, C. Liu and H. M. Cheng, *Nanotechnology*, 2009, **20**, 235707.
32 S. Hong, S. Jung, S. Kang, Y. Kim, X. Chen, S. Stankovich, *et al.*, *J. Nanosci. Nanotechnol.*, 2008, **8**, 424.
33 W. S. Hummers and R. E. Offeman, *J. Am. Chem. Soc.*, 1958, **80**, 1339.
34 V. D. Patake, S. S. Joshi, C. D. Lokhande and O. S. Joo, *Mater. Chem. Phys.*, 2009, **114**, 6.

 This journal is © The Royal Society of Chemistry 2017